CHAPTER 5

A MODEL FOR THE STRENGTH OF THE AS-DEPOSITED REGIONS OF LOW-ALLOY STEEL WELD METALS

5.1 NOMENCLATURE

The following nomenclature is used in this Chapter:

α	allotriomorphic ferrite
α_a	acicular ferrite
α_w	Widmanstätten ferrite
δ	delta-ferrite
$\Delta\sigma$	increment in yield stress
γ	austenite
ϵ	true strain
$\bar{\epsilon}$	true average strain
$\epsilon_{\mathrm{p}}^{\mathrm{I}}$	true plastic strain in softer phase of a dual-phase steel
$\epsilon_{\mathrm{p}}^{\mathrm{II}}$	true plastic strain in harder phase of a dual-phase steel
ϵ_{UTS}	true strain at ultimate tensile stress
ϵ_y	true strain at yielding
$\dot{\epsilon}$	strain rate
μ	shear modulus of iron-base solid-solution single crystal
τ_y	shear stress of iron-base solid-solution single crystal
σ	true stress
σ_α	microstructural strengthening due to allotriomorphic ferrite
σ_a	microstructural strengthening due to acicular ferrite
σ_{Fe}	yield strength of fully annealed pure iron as a function of temperature

and strain rate

σ_{micro} strengthening due to microstructure

σ_{micro_y} strengthening due to microstructure at the yield stress

$\sigma_{\text{micro}_{UTS}}$ strengthening due to microstructure at the ultimate tensile stress

σ_{SS_i} solid solution strengthening imparted due to an alloying element i

σ_{UTS} ultimate tensile stress

σ_w microstructural strengthening due to Widmanstätten ferrite

σ_y yield stress

Ω regression function defined in Eqn. 5.19

A area of cross-section of a tensile specimen

a, b regression coefficients used in the analysis of strength

C regression constant used in the analysis of strength

C_{equiv} carbon equivalent

i weld metal alloying element ($i = 1, \ldots, k$)

j number of weld analysed ($j = 1, \ldots, 35$)

K strength coefficient

K_α microstructural strength coefficient for allotriomorphic ferrite

K_a microstructural strength coefficient for acicular ferrite

K_w microstructural strength coefficient for Widmanstätten ferrite

n strain hardening exponent

n_α microstructural strain-hardening exponent for allotriomorphic ferrite

n_a microstructural strain-hardening exponent for acicular ferrite

n_w microstructural strain-hardening exponent for Widmanstätten ferrite

P applied load

T absolute temperature

V_α volume fraction of allotriomorphic ferrite in weld microstructure

V_a volume fraction of acicular ferrite in weld microstructure

V_w volume fraction of Widmanstätten ferrite in weld microstructure

V_{α_j} volume fraction of allotriomorphic ferrite in weld j

V_{a_j} volume fraction of acicular ferrite in weld j

V_{w_j} volume fraction of Widmanstätten ferrite in weld j

X Experimentally determined microstructural strengthening at the yield stress minus calculated microstructural strengthening at yield stress

$\bar{x}$ average carbon concentration in alloy

Y Experimentally determined microstructural strengthening at the ultimate tensile stress minus calculated microstructural strengthening at the ultimate tensile stress

5.2 INTRODUCTION

Much fundamental work has recently been done on the prediction of the microstructure of steel weld deposits (Bhadeshia *et al.*, 1985; Bhadeshia *et al.*, 1986; Svensson *et al.*, 1986), and it is now possible to estimate the as-welded microstructure as a function of chemical composition and thermal history. While the work on microstructure prediction has made good progress, it is the properties of welds which ultimately determine the quality of that weld. The aim of this work is to try and predict strength as a function of alloy concentration and microstructure, and also over a wide temperature range. Many welds are used or tested at non-ambient temperatures, and it is then not sufficient only to be able to predict their strength at room temperature.

The solidification of low-alloy steel weld deposits starts with the epitaxial growth of delta-ferrite (δ) from the parent plate grains at the fusion boundary. The high temperature gradients involved in arc welding cause solidification to proceed in a cellular manner with the grains having their major axes following the direction of maximum heat flow. On further cooling, allotriomorphs of austenite (γ) nucleate at the δ/δ cell boundaries, and anisotropic γ growth along these boundaries leads to the formation of columnar austenite grains which closely resemble the original δ-ferrite morphology. On cooling to temperatures below the Ae_3 temperature, the first phase to form is allotriomorphic ferrite (α). The fer-

rite nucleates at the columnar austenite grain boundaries, which rapidly become covered with a nearly uniform layer of α. Following this, Widmanstätten ferrite (α_w) nucleates at the α/γ boundaries and grows by a displacive mechanism in the form of thin, wedge-shaped plates at a rate approximately controlled by the diffusion of carbon in the austenite ahead of the interface. At the same time, a third phase, acicular ferrite (α_a), which consists of a series of non-parallel arrays of bainite laths, nucleates intragranularly (Yang and Bhadeshia, 1986; Bhadeshia, 1987). Finally, very small volume fractions of "microphases" are found within the acicular ferrite consisting of mixtures of martensite, degenerate pearlite and retained austenite, all resulting from the austenite remaining untransformed after α, α_w, and α_a have formed. However, microphases comprise typically only 1–3% of the weld microstructure, and it is the three morphologically distinct phases –allotriomorphic, Widmanstätten, and acicular ferrite– which can be said to form the primary microstructure (Bhadeshia *et al.*, 1985).

5.3 METHOD

It is normal practice to express the weld metal strength as a function of the alloying elements present. Equations used in such analyses typically state the yield stress as follows:

$$\sigma_y = \mathrm{C} + a\ \mathrm{wt\%Mn} + b\ \mathrm{wt\%Si} + \ldots \tag{5.1}$$

where C is a constant,

and a, b, ... are supposed to define the role of alloying additions (Bailey and Pargeter, 1978; Bosward and John, 1979; Evans, 1981).

Identical equations have been derived to allow for the estimation of the microstructure of the ultimate tensile strength of a weld, σ_{UTS} (Bailey and Pargeter, 1978; Samuel, 1984). C and the other coefficients are found by regression analysis on a given set of data, and, as such, are highly specific to that set of data, and doubtful in extrapolation. This approach is inadequate, as shown by a wide spread of coefficients obtained by different workers for the strengthening effects of individual elements, (summarised by Judson (1982), and Abson and Pargeter (1986)). (The diversity is hardly surprising, since the weld strength is a function

of the heat input, interpass temperature, columnar grain size, dislocation density, *&c.*). More importantly, such an equation ignores the effects of thermal history since the microstructural reheating that occurs during multi-pass welding, and also post-weld heat treatment, does not change the composition of a weld, and yet alters its strength. The strength clearly must also be a function of the microstructure. Most welding variables (*e.g.* heat input, preheat temperature, welding geometry), manifest themselves in altering the microstructure. Also, it does not allow for any means by which the strength of a weld at yield and at UTS may be related.

In a multi-phase system, such as a weld deposit, the overall strength will be strongly related to the strengths and volume fractions of the phases present, an optimum high strength, high toughness, microstructure being associated with a high proportion of acicular ferrite. The simplest assumption from this would be that the mean strength of the weld should be linearly related to the strengths and abundances of the phases present (see, for example, Tweed and Knott, 1987a). This "rule of mixtures" is most commonly used for predicting the strength of composite materials, when a ductile matrix is reinforced by brittle (Kelly, 1966), or even ductile (Ahmad and Barranco, 1970; Davis and Scala, 1973), continuous fibres, although strictly the rule shows the upper bound of the strength since the fibres and the matrix are assumed to fail simultaneously (Fukuda *et al.*, 1981).

The following model is based on the assumption that the strength can be factorised into components due to the intrinsic strength of iron, solid solution strengthening, and the contributions from the three major phases (α, α_w, α_a) which constitute the microstructure:

$$\sigma = \sigma_{\mathrm{Fe}} + \sum_{i=1}^{k} \sigma_{\mathrm{SS}_i} + \sigma_{\mathrm{micro}} \tag{5.2}$$

where σ_{Fe} is the strength of fully annealed pure iron as a function of temperature and strain rate,

σ_{SS_i} is the solid solution strengthening due to an alloying element i, †

† Allotriomorphic ferrite appears in weld deposits to grow without the redis-

and σ_{micro} is the strengthening due to microstructure.

Substituting for σ_{micro}, Eqn. 5.2 may be written,

$$\sigma = \sigma_{\text{Fe}} + \sum_{i=1}^{k} \sigma_{\text{SS}_i} + V_\alpha \sigma_\alpha + V_w \sigma_w + V_a \sigma_a \tag{5.3}$$

where V_α, V_a, and V_w are the volume fractions of the allotriomorphic, acicular, and Widmanstätten ferrite phases respectively.

To express the stress as a function of strain, it is assumed that the true stress/true strain curve in the plastic region can be approximated by (Nadai, 1931)

$$\sigma = K\epsilon^n \tag{5.4}$$

where ϵ is the true strain

n is the strain hardening exponent

and K is the strength coefficient, equal to the value of the flow stress at $\epsilon^n = 1.0$.

This equation describes a state of stable plastic deformation, and, although alternative descriptions exist, it is this equation which has been most successfully applied by various workers to describing weld metal tensile behaviour in this regime (Tweed, 1987b; McRobie and Knott, 1985).

Using this relationship, Eqn. 5.3 has been further extended to become

---

tribution of substitutional alloying elements during transformation (Bhadeshia *et al.*, 1985), α_w grows by a paraequilibrium mechanism (Bhadeshia, 1987), and α_a growth is diffusionless (Yang and Bhadeshia, 1986; Strangwood and Bhadeshia, 1986) with subsequent rejection of carbon into the residual austenite. This means that the solid solution strengthening contribution from substitutional elements is identical for all three phases.

$$\sigma = \sigma_{\mathrm{Fe}} + \sum_{i=1}^{k} \sigma_{\mathrm{SS}_i} + V_\alpha K_\alpha \epsilon^{n_\alpha} + V_w K_w \epsilon^{n_w} + V_a K_a \epsilon^{n_a} \qquad (5.5)$$

where K_α, K_w, and K_a are strength coefficients, and n_α, n_w, and n_a are strain-hardening exponents for allotriomorphic ferrite, Widmanstätten ferrite, and acicular ferrite respectively.

Since the layers of allotriomorphic ferrite that grow at the γ grain boundaries do not usually extend very far into the grains of austenite, the assumption is made that the allotriomorphic ferrite grain size, as limited by hard impingement along the γ grain boundaries, does not vary significantly between welds in low-alloy steels. The plate morphologies of α_w and α_a are generated by displacive transformation, and it is also assumed that any variations in their sizes are not significant, relevant to the other variables (Bhadeshia and Svensson, 1988). The austenite grain size is ignored in this calculation because the grains are usually too large to contribute significantly to strength.

In order to calculate the strength of pure iron, σ_{Fe}, and the effect of alloying elements on solid solution strengthening, σ_{SS}, published data have been collected for the temperature range 100–750K. Data for the normal yield stress of pure annealed polycrystalline b.c.c. iron as a function of strain rate and temperature have been taken from three sources (Conrad and Fredrick, 1962; Altshuler and Christian, 1967; Kimura *et al.*, 1981). The individual effects of five ferrous alloying elements (Mn, Si, Ni, Cr, and Co) on the yield strength of pure iron as a function of concentration and temperature are obtained from work due to Leslie (1972), and information on the effect of nitrogen on the strength of high purity iron, as a function of temperature (at a strain rate similar to that used by Leslie), is obtained from the work of Kitajima *et al.* (1979). The detailed data were represented on computer as cubic splines which allow a continuous representation of σ_{SS} with temperature (Hayes, 1974). Thus although in this work only room temperature strength is considered, in fact, σ_{SS} can now be estimated from 100 to 750K. Nitrogen is assumed to be in solid solution, and strain ageing effects in the as-welded microstructure are taken as negligible. It should be noted that many elements, such as nickel, manganese, and nitrogen, give *softening* at certain concentrations and

temperatures. This occurs because distortion of the atomic lattice, particularly at low temperatures, can locally reduce the Peierls-Nabarro barrier and facilitate slip.

The solid solution strengthening of iron at 298K has been determined for phosphorus (Leslie, 1972), molybdenum, aluminium, and vanadium (Takeuchi, 1969), titanium (Takeuchi *et al.*, 1968), and boron (Irvine and Pickering, 1963), and, in the absence of further data, the strengthening due to these elements is taken to be athermal. Although this is a simplification, it is not a serious one since it has become apparent from this work that typically not less than 90% of the solid solution strengthening in a low-alloy steel weld deposit is due to manganese, silicon, and nitrogen. Where necessary, shear yield stress data were converted into normal yield stress data using the Tresca criterion (Dieter, 1976) †.

The effect of carbon on the strength of ferrite has been investigated by Chilton and Kelly (1968), and Norström (1976). However, the solubility of carbon in ferrite in contact with cementite decreases with temperature, and at room temperature is less than 10^{-3}at% (Hansen, 1958), and consequently the solid solution strengthening due to carbon need only be included for temperatures greater than 200°C. In fact, during the cooling of a weld, the ferrite grows in contact with austenite rather than cementite, so that it is the solubility with respect to cementite that needs to be considered, but this is not expected to be very different (Bhadeshia, 1982). Oxygen and sulphur are assumed to be present in the form of inclusions, and not to be in solid solution (Steel, 1972).

Although data for a variety of strain rates had been collated, (typically in the range $5.0\text{x}10^{-6}$ to 10^{-2}s^{-1}), for the following work a value of $2.5\text{x}10^{-4}\text{s}^{-1}$, as used by Leslie, was chosen. A listout of the program written to allow the calculation of σ_{Fe} and $\sum_{i=1}^{k} \sigma_{SS_i}$ as a function of temperature is given in Appendix 3.

In order to calculate σ_α, σ_a, and σ_w, data on 35 welds was taken from four sources [Widgery (1976), Bailey and Pargeter (1978), Cunha *et al.* (1982), and Dowling *et al.*, (1986)] for which experimental results for yield stress and ultimate tensile stress from primary (unrefined) all-weld metal specimens were given, together with the volume fractions of α, α_w, and α_a comprising them. The welding conditions are all different, but these differences are all taken into account, since

† Popular earlier data from Lacy and Gensamer (1944) were not used since the interstitial content of their alloys was not rigorously controlled.

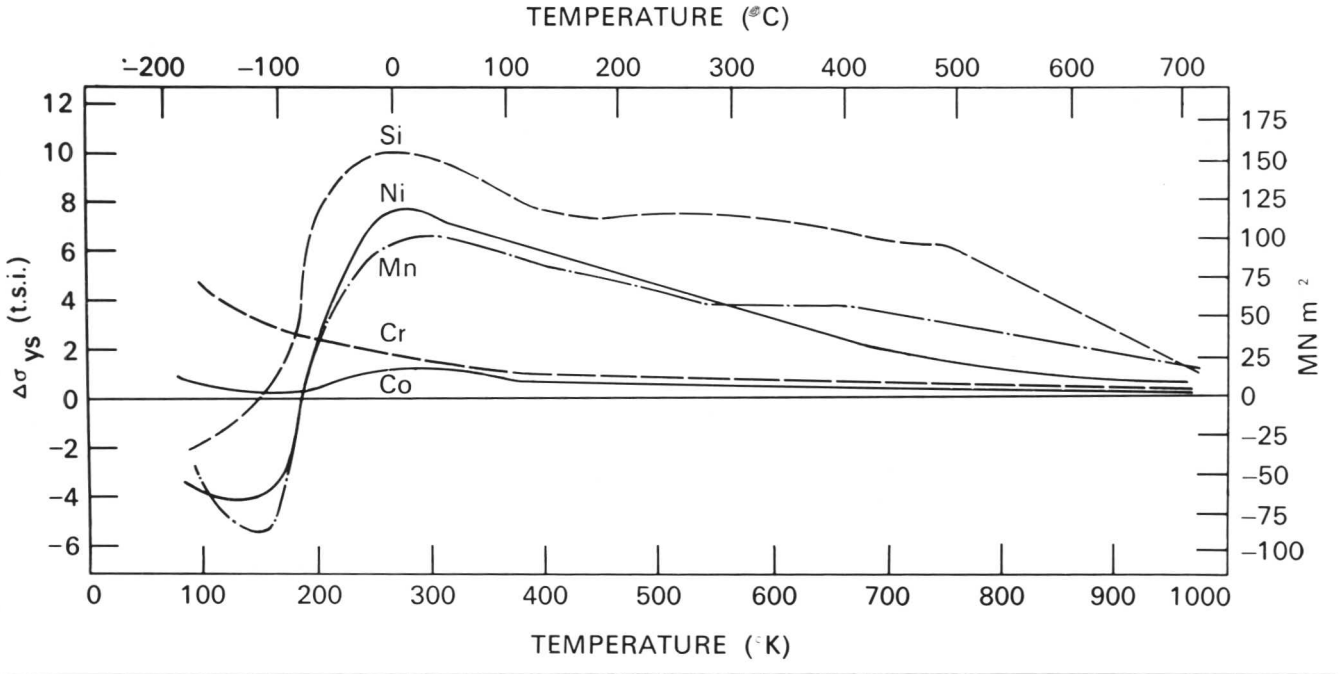

Figure 5.1: Effect of solutes on the strength of polycrystalline iron as a function of temperature for 3 at.% concentration of solutes.

$\Delta\sigma$ = increment in yield stress. ($\dot{\epsilon} = 2.5 \times 10^{-4}$/s).

One of a series of graphs given by Leslie, W. C. (1972), *Metall. Trans.*, **3**, 5-26.

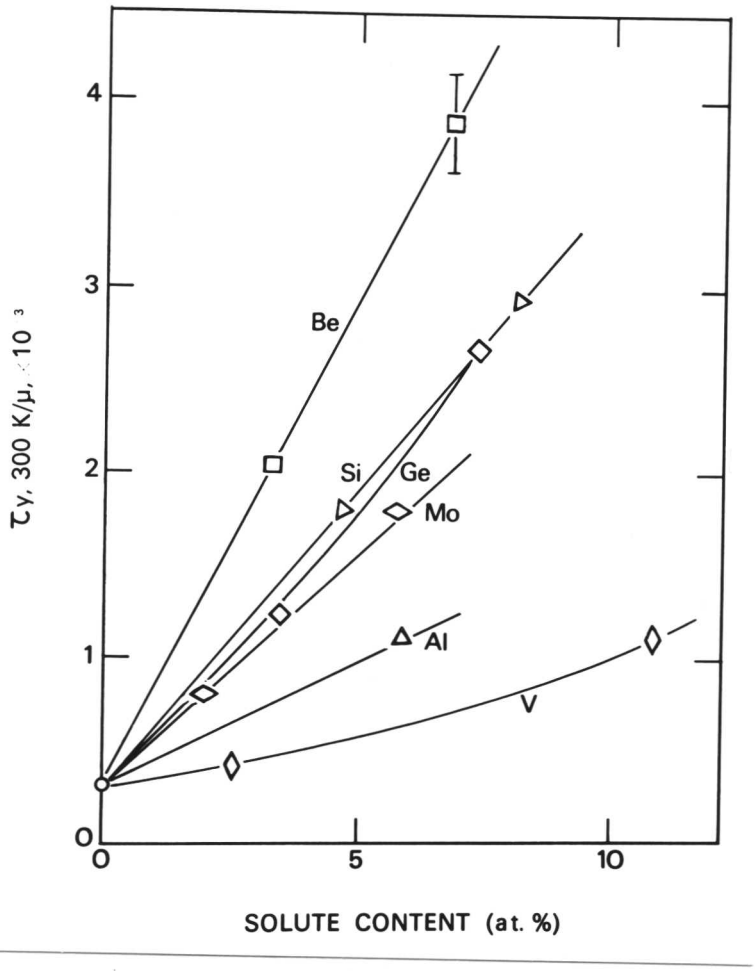

Figure 5.2: Strength of iron-base solid solution single crystals; the ratio of the resolved shear stress at the lower yield point to shear modulus as a function of atomic concentration of solute. (After Takeuchi, S. (1969), *J. Phys. Soc. Japan*, **27**, 167).

they cause different resulting microstructures.

From Eqn. 5.2, the strenghening due to microstructure at the yield stress

$$\sigma_{\text{micro}_y} = \sigma_y - \sigma_{\text{Fe}} - \sum_{i=1}^{k} \sigma_{\text{SS}_i} \tag{5.6a}$$

where σ_y is the yield stress.

Similarly

$$\sigma_{\text{micro}_{UTS}} = \sigma_{UTS} - \sigma_{\text{Fe}} - \sum_{i=1}^{k} \sigma_{\text{SS}_i} \tag{5.6b}$$

where σ_{UTS} is the ultimate tensile stress.

At the yield stress

$$\sigma_{\text{micro}_y} = V_\alpha K_\alpha (\epsilon_y)^{n_\alpha} + V_w K_w (\epsilon_y)^{n_w} + V_a K_a (\epsilon_y)^{n_a} \tag{5.7}$$

where ϵ_y is the true strain at yielding.

Since proof stress is usually measured at 0.2% plastic strain, a fair assumption for ϵ_y is to take it as corresponding to the point of 0.2% plastic strain. Accordingly, ϵ_y was taken as 0.002.

The ultimate tensile strength should now be considered. The onset of necking corresponds to the transition from smooth necking to local fracture and may be defined by the Considère construction (Considère, 1885).

The true stress

$$\sigma = \frac{P}{A} \tag{5.8}$$

where P is the applied load

and A is the area of cross-section of the tensile specimen.

Necking occurs when an increase in strain produces no increase in load, *i.e.* $dP = 0$

Therefore, from Eqn. 5.8

$$dP = A\,d\sigma + \sigma\,dA = 0 \tag{5.9}$$

Therefore

$$\frac{d\sigma}{\sigma} = \frac{-dA}{A} \tag{5.10}$$

During deformation, the volume of the specimen is taken as constant, *i.e.*

$$d(Al) = A\,dl + l\,dA = 0 \tag{5.11}$$

Therefore

$$\frac{dl}{l} = \frac{-dA}{A} \equiv d\epsilon \tag{5.12}$$

Combining Eqns. 5.10 and 5.12 gives

$$\frac{d\sigma}{d\epsilon} = \sigma \tag{5.13}$$

For $\sigma = K\epsilon^n$, therefore, Eqn. 5.13 means

$$\frac{d\sigma}{d\epsilon} = nK\epsilon^{n-1} = K\epsilon^n \tag{5.14}$$

Therefore

$$\epsilon = n \tag{5.15}$$

Therefore, necking occurs when the true strain equals the strain-hardening exponent. Thus, the strengthening due to microstructure at the utimate tensile strength, $\sigma_{\text{micro}_{UTS}}$, may be written

$$\sigma_{\text{micro}_{UTS}} = V_\alpha K_\alpha (n_\alpha)^{n_\alpha} + V_w K_w (n_w)^{n_w} + V_a K_a (n_a)^{n_a} \tag{5.16}$$

It should be emphasized that the coefficients K_α, K_w, and K_a, and n_α, n_w, and n_a are not directly comparable to the coefficients K and n in Eqn. 5.4, since the strengthening due to pure annealed iron, and that due to microstructure has been removed. The different values of strain in the three phases takes into account that the post-yield strain will *not* be uniformly distributed, with the harder constituents deforming less (Tomota *et al.*, 1976; Tweed and Knott, 1987b). Realistically, the phases have different yield strengths and deformation should be inhomogeneous. However, in the absence of detailed data on the deformation characteristics of the individual phases, and on the grounds that the phases are not too dissimilar, we assume that the strain in any phase is the same as the average overall sample strain, *i.e.* deformation is homogeneous. For example, Figure 5.3 shows the case calculated for a ferrite/martensite dual-phase steel, when the mechanical properties of the constituent phases are quite different. It can be seen that although the initial strain increments (as a function of the average strain, $\bar{\epsilon}$) are quite different in the two phases, as the softer phase work-hardens, the rate of straining in the two phases becomes about equal. Since the true strain at the ultimate tensile stress is very much greater than the true strain at yielding, it is a good approximation to assume homogeneous deformation at the ultimate tensile stress, although near the yield point it is very likely that the softest of the phases will yield first.

The data used give experimentally determined values σ_{micro_y}, $\sigma_{\text{micro}_{UTS}}$, V_α, V_w, and V_a. For a given weld, let

$$X = \sigma_{\text{micro}_y} - V_\alpha K_\alpha (0.002)^{n_\alpha} - V_w K_w (0.002)^{n_w} - V_a K_a (0.002)^{n_a} \tag{5.17}$$

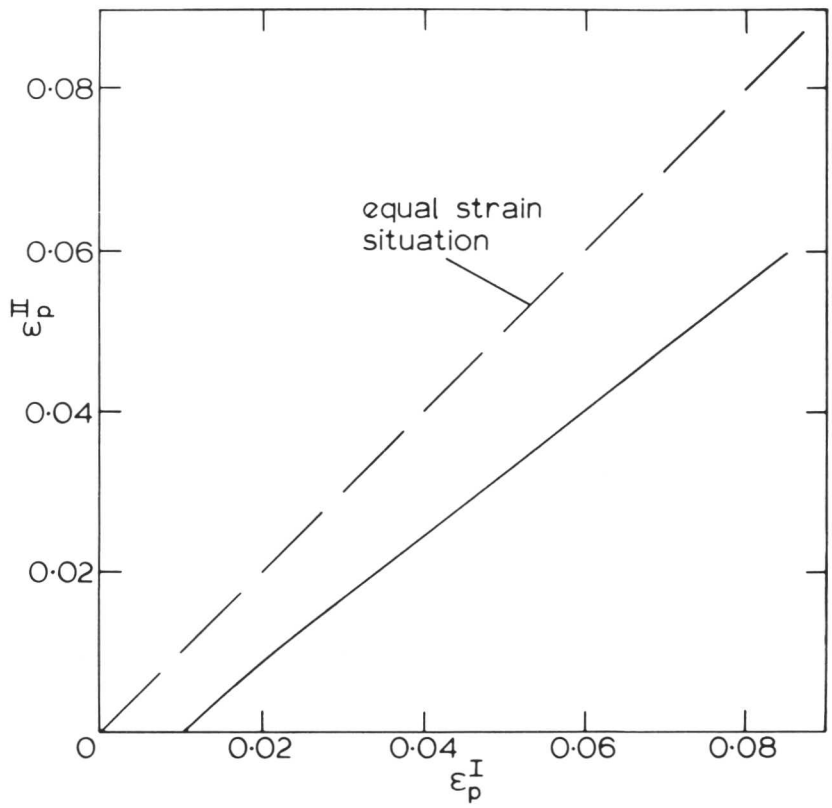

Figure 5.3: Calculated cumulative plastic strain in hard phase, ϵ_p^{II}, versus that in the soft phase, ϵ_p^I for ferrite/martensite dual-phase steel. (After H. K. D. H. Bhadeshia and D. V. Edmonds, *Met. Sci.*, **14**, (2), 41-49).

Reference	Designated	σ_y	σ_{UTS}	$\sigma_{\text{Fe}} + \sum_{i=1}^{k} \sigma_{\text{SS}_i}$	σ_{micro_y}	$\sigma_{\text{micro}_{UTS}}$
	Weld ID.	MPa	MPa	MPa	MPa	MPa
Widgery, 1976	D	563	696	336	227	360
"	J2R	503	604	295	208	309
"	J2RR	504	608	299	205	309
"	O	569	689	364	205	325
"	Q	582	710	289	293	421
"	R	547	650	325	222	325
"	S	569	734	346	223	388
"	U	573	714	377	196	337
"	X	535	630	316	219	314
"	Y	560	692	311	249	381
Bailey and Pargeter, 1978	31	405	580	303	102	277
"	63	405	560	361	108	263
"	29	440	600	274	166	326
"	23	375	505	277	98	228
"	25	400	525	263	137	262
"	59	425	575	318	107	257
"	27	345	480	256	88	223
"	33	370	520	264	106	256
"	35	435	560	271	164	289
"	61	420	530	279	141	251
"	37	415	545	265	149	279
"	39	425	565	273	152	292
"	41	385	530	265	120	265
"	67	425	560	265	160	295
Cunha *et al.*, 1982	13	421	504	297	124	207
"	14	631	726	309	322	417
"	15	540	645	324	216	321
"	16	484	587	287	197	300
"	17	537	628	295	242	333
"	18	453	596	283	170	313
"	19	520	593	270	250	323
Dowling *et al.*, 1986	B1	624	657	259	365	398
"	B4	618	668	262	356	406
"	K6	627	661	275	352	386
"	K8	599	699	290	309	409

Table 5.1: Calculation of σ_{micro_y} and $\sigma_{\text{micro}_{UTS}}$ for welds used in the analysis of strain hardening coefficients.

Weld No.	σ_{micro_y}	$\sigma_{\text{micro}_{UTS}}$	V_α	V_w	V_a
D	227	360	0.17	0.01	0.82
J2R	208	309	0.31	0.04	0.65
J2RR	205	309	0.25	0.01	0.74
O	205	325	0.16	0.02	0.82
Q	293	421	0.02	0.02	0.96
R	222	325	0.22	0.04	0.745
S	223	388	0.09	0.02	0.89
U	196	337	0.29	0.02	0.69
X	219	314	0.24	0.0	0.76
Y	249	381	0.12	0.01	0.87
31	102	277	0.43	0.22	0.35
63	108	263	0.44	0.31	0.25
29	166	326	0.40	0.08	0.52
23	98	228	0.45	0.27	0.28
25	137	262	0.24	0.18	0.58
59	107	257	0.35	0.21	0.44
27	88	223	0.37	0.21	0.42
33	106	256	0.39	0.25	0.36
35	164	289	0.38	0.10	0.52
61	141	251	0.39	0.08	0.53
37	149	279	0.37	0.25	0.38
39	152	292	0.29	0.24	0.47
41	120	265	0.41	0.16	0.43
67	160	295	0.46	0.08	0.46
13	124	207	0.35	0.24	0.41
14	322	417	0.08	0.92	0.0
15	216	321	0.18	0.03	0.79
16	197	300	0.25	0.18	0.57
17	242	333	0.24	0.07	0.69
18	170	313	0.22	0.07	0.71
19	250	323	0.36	0.44	0.20
B1	365	398	0.0	0.0	1.0
B4	356	406	0.0	0.0	1.0
K6	352	386	0.11	0.0	0.89
K8	309	409	0.05	0.03	0.92

Table 5.2: Summary of σ_{micro_y} and $\sigma_{\text{micro}_{UTS}}$ together with volume fractions of phases present in the welds.

and let

$$Y = \sigma_{\text{micro}_{UTS}} - V_\alpha K_\alpha (n_\alpha)^{n_\alpha} - V_w K_w (n_w)^{n_w} - V_a K_a (n_a)^{n_a} \tag{5.18}$$

Eqn. 5.16 defines the condition that all phases achieve plastic instability at the same strain at which the sample as a whole begins to neck. The values of K_α, n_α, *&c.* thus obtained will reflect the different hardening rates necessary in order to satisfy this condition, so that it is expected that the allotriomorphic ferrite, which starts off relatively weak should have a high value of strain-hardening exponent, n_α.

By the least squares method, and giving the values for σ_{micro_y} and $\sigma_{\text{micro}_{UTS}}$ equal weightings, the best fit for the data is when the function Ω is a minimum, where

$$\Omega\{K_\alpha, K_w, K_a, n_\alpha, n_w, n_a\} = \sum_{j=1}^{35} X^2 + \sum_{j=1}^{35} Y^2 \tag{5.19}$$

where j is the number of sets of data analysed ($j = 1, \ldots, 35$).

This minimum can be found by taking the partial derivatives of Eqn. 5.14 with respect to K_α, K_w, K_a, n_α, n_w, and n_a as follows:

$$\frac{\partial \Omega}{\partial K_\alpha} = 2 \sum_{j=1}^{35} \{X.V_{\alpha_i} (0.002)^{n_\alpha}\} + 2 \sum_{j=1}^{35} \{Y.V_{\alpha_i} (n_\alpha)^{n_\alpha}\} \tag{5.20a}$$

$$\frac{\partial \Omega}{\partial K_w} = 2 \sum_{j=1}^{35} \{X.V_{w_i} (0.002)^{n_w}\} + 2 \sum_{j=1}^{35} \{Y.V_{w_i} (n_w)^{n_w}\} \tag{5.20b}$$

$$\frac{\partial \Omega}{\partial K_a} = 2 \sum_{j=1}^{35} \{X.V_a (0.002)^{n_a}\} + 2 \sum_{j=1}^{35} \{Y.V_{a_i} (n_a)^{n_a}\} \tag{5.20c}$$

$$\frac{\partial \Omega}{\partial n_\alpha} = 2 \sum_{j=1}^{35} \{X.V_{\alpha_i} K_\alpha \ln(0.002).(0.002)^{n_\alpha}\}$$

$$+ 2 \sum_{j=1}^{35} [Y.V_{\alpha_i} K_\alpha (n_\alpha)^{n_\alpha} \{1 + \ln(n_\alpha)\}] \qquad (5.20d)$$

$$\frac{\partial \Omega}{\partial n_w} = 2 \sum_{j=1}^{35} \{X.V_{w_i} K_w \ln(0.002).(0.002)^{n_w}\}$$

$$+ 2 \sum_{j=1}^{35} [Y.V_{w_i} K_w (n_w)^{n_w} \{1 + \ln(n_w)\}] \qquad (5.20e)$$

$$\frac{\partial \Omega}{\partial n_a} = 2 \sum_{j=1}^{35} \{X.V_{a_i} K_a \ln(0.002).(0.002)^{n_a}\}$$

$$+ 2 \sum_{j=1}^{35} [Y.V_{a_i} K_a (n_a)^{n_a} \{1 + \ln(n_a)\}] \qquad (5.20f)$$

Eqns. 5.15a-f will all equal zero when a valid solution is obtained. In order to find this condition, a NAG† FORTRAN subroutine was used which estimates partial derivatives of the functions supplied from their arguments, and uses these to rapidly reach the solution nearest to a set of supplied "best guess" values. This achieved using a convergence technique described elsewhere (Powell, 1970).

5.4 CHOICE OF GUESSED VALUES

Since Eqns. 5.15a-f were non-linear, there would be more than one solution for the equations, and so the selection of the initial guess values would be extremely important. Welds Q and 14, which have very high percentages of acicular ferrite and Widmanstätten ferrite respectively (see Table 5.2) were treated as single phase microstructures, and knowing σ_y, σ_{UTS}, and $\sum_{i=1}^{k} \sigma_{SS_i}$, values for K_w, n_w, K_a, and n_a were found using Eqn. 5.5. K_α and n_α were then found by substituting

† ©National Algorithms Group Ltd., 256 Banbury Road, Oxford, U.K.

these approximate values into Eqn. 5.5 using the data for weld 67, which contains 46% α. The values thus derived are as follows:

$$\begin{aligned} K_\alpha &= 202 \text{ MPa} & n_\alpha &= 0.595 \\ K_w &= 504 \text{ MPa} & n_w &= 0.072 \\ K_a &= 526 \text{ MPa} & n_a &= 0.094 \end{aligned}$$

5.5 RESULTS

After 22 iterations, the arguments of Eqns. 5.20a-f were all less than 10^{-6}, and the following values for the coefficients were obtained:

$$\begin{aligned} K_\alpha &= 124 \text{ MPa} & n_\alpha &= 0.644 \\ K_w &= 478 \text{ MPa} & n_w &= 0.0812 \\ K_a &= 499 \text{ MPa} & n_a &= 0.103 \end{aligned}$$

Substituting in Eqn. 5.5 gives two general equations:

$$\sigma_{\text{micro}_y} = 2.26V_\alpha + 289V_w + 263V_a \tag{5.21a}$$

$$\sigma_{\text{micro}_{UTS}} = 94V_\alpha + 390V_w + 395V_a \tag{5.21b}$$

More generally, the overall strength of a weld may be written:

$$\sigma = \sigma_{\text{Fe}} + \sum_{i=1}^{k} \sigma_{\text{SS}_i} + V_\alpha.124\epsilon^{0.644} + V_w.478\epsilon^{0.0812} + V_a.499\epsilon^{0.103} \tag{5.22}$$

Measured and calculated values for yield strength and ultimate tensile strength for the 35 welds are plotted in Figures 5.4 and 5.5 respectively.

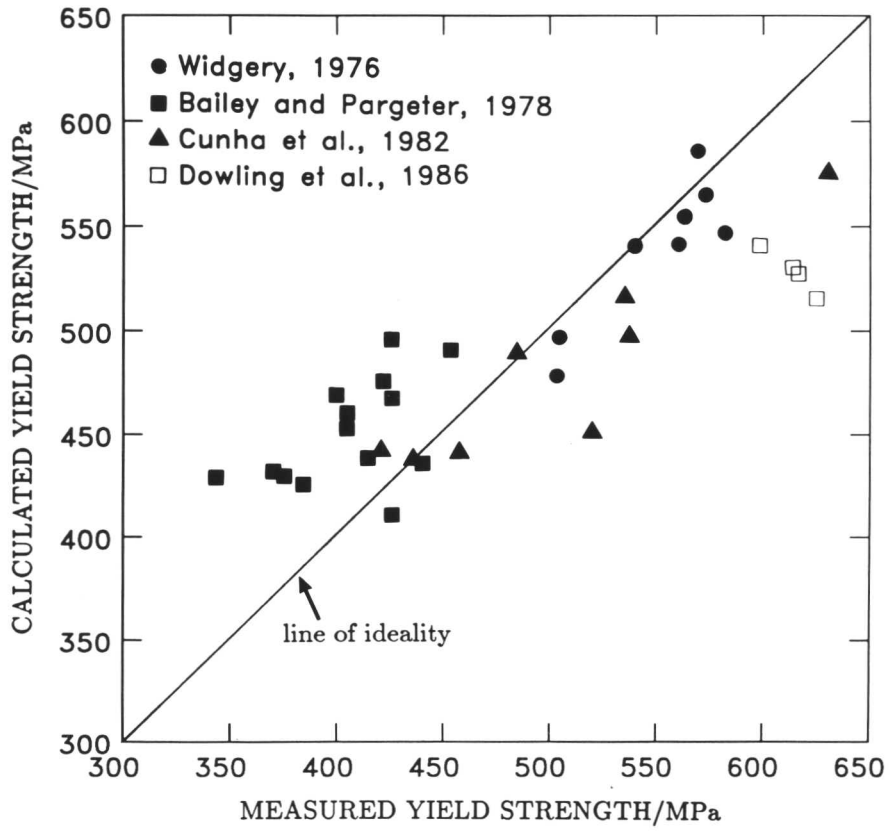

Figure 5.4: Measured values for yield strength plotted against values predicted using Eqn. 5.21a. (Correlation coefficient = 0.85).

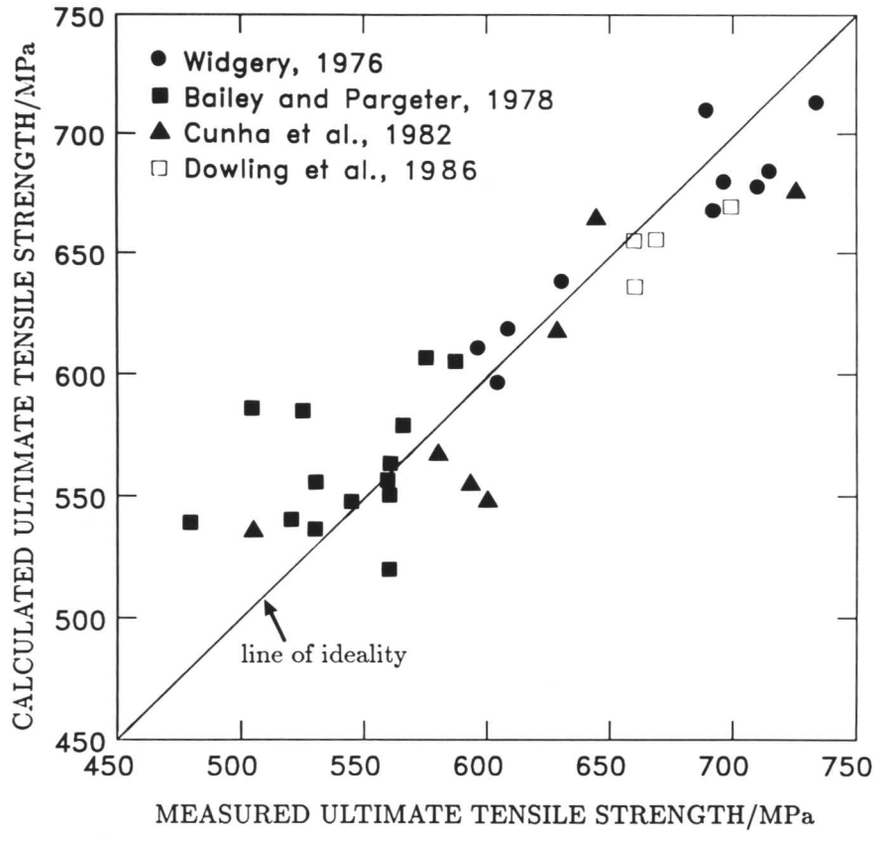

Figure 5.5: Measured and predicted values for ultimate tensile strength. (Correlation coefficient = 0.91).

5.6 USING THE MODEL

Figures 5.4 and 5.5 show that the overall ability of the equations to predict the tensile strength of the as-deposited regions of a wide variety of welds and welding conditions is very good. It can be seen from Eqn. 5.21a that allotriomorphic ferrite has a yield strength only a little greater than that of pure iron, whereas acicular ferrite and Widmanstätten ferrite are much stronger. Widmanstätten ferrite is expected to be stronger than allotriomorphic ferrite. α_w grows by a displacive transformation mechanism, and should have a higher dislocation density (Bhadeshia, 1981). Furthermore, Widmanstätten ferrite laths in weld deposits typically have carbides aligned along them, and these will contribute to the strength. The microphases present in acicular ferrite would contribute to the strength of α_a in a similar way. Although, allotriomorphic ferrite work-hardens much more than Widmanstätten ferrite and acicular ferrite with $n_\alpha \gg n_a > n_w$, its strength at UTS is still much less than that of the other two phases whose microstructural contributions are effectively identical. It should be noted that to predict weld metal yield stress and ultimate tensile stress is of potential use in fatigue analysis, since the ratio between the two will give an indication of susceptibility to fatigue crack propagation (A. S. M., 1985).

Figure 5.6 shows the true stress/true strain curve for a hypothetical Fe-0.06C-0.35Si-1.0Mn wt% weld metal microstructure containing equal volume fractions of allotriomorphic ferrite, Widmanstätten ferrite, and acicular ferrite, calculated using Eqn. 5.22. The figure illustrates how the relative strengthening contributions of the three phases alter during plastic deformation. It can be seen that allotriomorphic ferrite provides little strengthening in the early stages of plastic deformation, but work-hardens rapidly as deformation progresses to contribute appreciably to the overall strength. Note that the relatively large plasic strains have caused the elastic region to be compressed into the y axis. Such results provide an explanation for the recent experimental observations of Oldland (1985), who worked on low-alloy C-Mn and C-Mn-Nb SA weld metals containing up to 60% allotriomorphic ferrite, and noted that weld metal yield strength and ultimate tensile strength correlated strongly with the volume fraction of allotriomorphic ferrite present in the welds. This can be appreciated quantitatively from Eqns. 5.21a and b, where a small change in V_α will lead to a large change in observed strength.

In order to demonstrate the general applicability of the model for strength, the

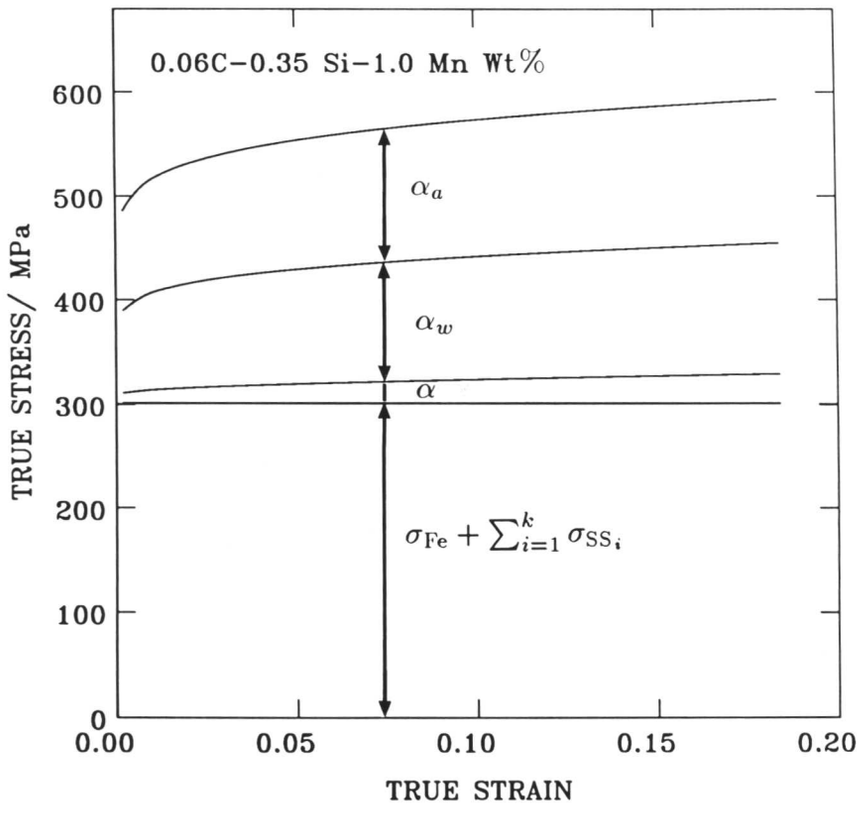

Figure 5.6: Calculated true stress/true strain curves up to the ultimate tensile stress for a weld metal with a composition Fe-0.06C-0.35Si-1.0Mn wt% comprising one third allotriomorphic ferrite, Widmanstätten ferrite, and acicular ferrite.

tensile behaviour of a series of low-alloy C-Mn welds containing 0.35 wt% Si, with systematically varying carbon and manganese concentrations has been calculated using volume fractions which are themselves calculated using the phase transformations model for the calculation of weld metal microstructure described earlier (Bhadeshia *et al.*, 1985). Precise details of the calculation of the volume fractions of the phases in the welds described are given in Bhadeshia and Svensson (1988). The carbon and manganese contents were chosen, together with the fixed percentage of silicon, to reflect simple nominal chemical compositions that might be typical of low-alloy steel weld deposits, although, in fact, the model is able to accommodate all of the major elements that are commonly found in low C-Mn weld metals. Figures 5.7a and b show how the yield stress and ultimate tensile stress vary with manganese content for different carbon concentrations. The results are extremely interesting. First of all, it can be seen that additions of both manganese and carbon will lead to an increase in weld metal tensile strength. Manganese provides solid solution strengthening, and both manganese and carbon act to increase the size of the austenite phase field, and so reduce the driving force for ferrite formation at any given temperature. This behaviour promotes the formation of acicular ferrite, at the expense of allotriomorphic ferrite, and also Widmanstätten ferrite. It can also be seen how the change from 0.03 wt% C to 0.06 wt% C leads to a much greater increase in tensile strength than when going from 0.06 wt% C to 0.10 wt% C. This explanation for this is that as the carbon concentration decreases to low levels, the kinetics of the allotriomorphic ferrite transformation increase rapidly. The concentration profile of the carbon ahead of the advancing interface is strongly dependent upon $\bar{x}$, the average carbon concentration in the alloy, and becomes very steep (*i.e.* diffusion away from the interface becomes very rapid) as the carbon concentration tends to zero. Thus, increasing the carbon content from 0.03 wt% C 0.06 wt% C has a much greater effect upon the ultimate volume fraction of allotriomorphic ferrite, and so mechanical properties, than increments at higher carbon concentrations.

This observation provides an answer as to why two empirical different carbon equivalent equations have emerged over the years. The carbon equivalent of a steel is a measure of its weldability, and is most usually calculated as follows (Easterling, 1983):

a)

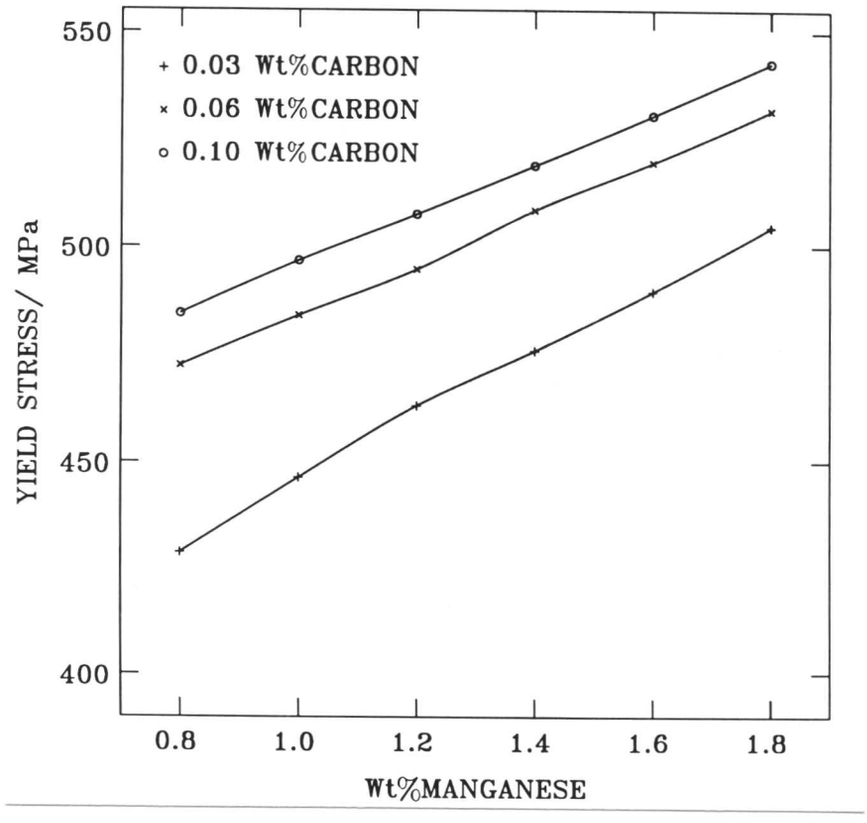

b)

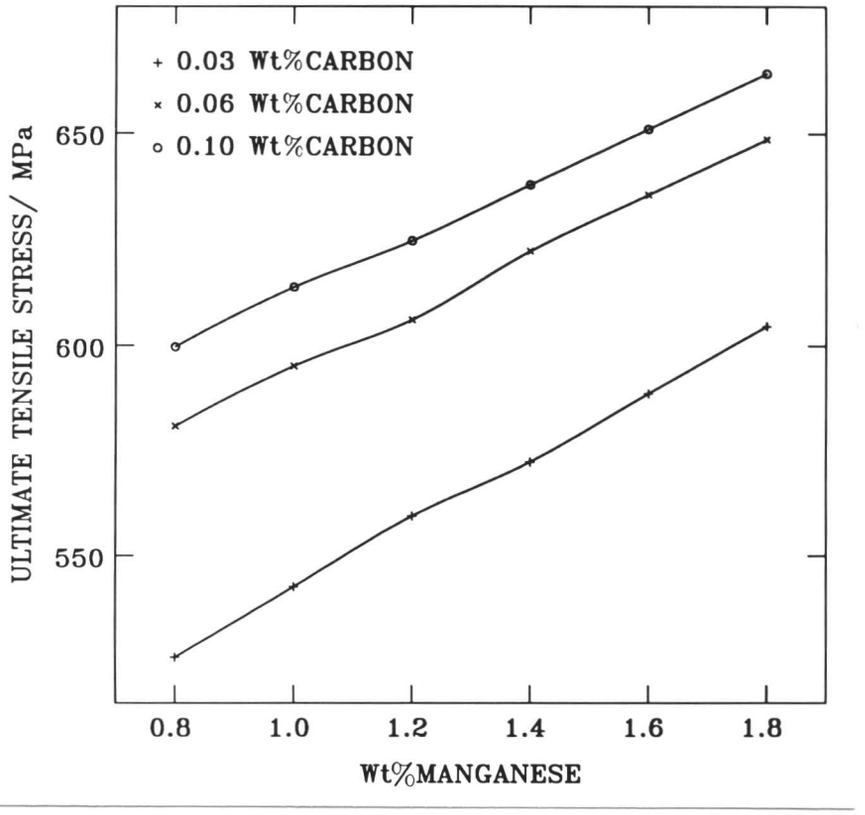

Figures 5.7a and b: Calculation of (a) yield stress, and (b) ultimate tensile stress for a series of hypothetical welds deposited in the flat position. (Nominal heat input = 1 kJ/mm). The welds contain 0.35wt% Si, and varying concentrations of carbon and manganese.

$$C_{\text{equiv}} = \text{C} + \frac{\text{Mn}}{6} + \frac{\text{Cr} + \text{Mo} + \text{V}}{5} + \frac{\text{Cu} + \text{Ni}}{15} \qquad (5.23)$$

This equation describes approximately how the alloying elements present will alter the transformation behaviour of the steel during welding, and it is generally supposed that a steel will be weldable if $C_{\text{equiv}} < 0.4$. At low carbon concentrations, however, Eqn. 5.22 is found to be unreliable, and an empirical equation due to Ito and Bessayo (1968) is preferred:

$$C_{\text{equiv}} = \text{C} + \frac{\text{Mn} + \text{Cu} + \text{Cr}}{20} + \frac{\text{Si}}{30} + \frac{\text{V}}{10} + \frac{\text{Mo}}{15} + \frac{\text{Ni}}{60} + 5\text{B} \qquad (5.24)$$

It can be immediately seen that the apparent influence of substitutional alloying elements on weldability is been found to be much less for low-carbon steels as indicated by the larger denominators in Eqn. 5.23. This can be understood in terms of the greatly increased potency of carbon additions at low carbon concentrations, when the influence of substitutional alloying elements on weldability *relative to that of carbon* is correspondingly reduced. At higher carbon concentrations, they have a more noticeable effect.

Figures 5.8a and b plot the true stress/true strain curve for a set of welds with varying manganese and carbon concentrations. The strain experienced during uniform deformation is readily calculable from σ_y up to the ultimate tensile stress. The ultimate tensile stress is calculated from the criterion specified in Eqn. 5.18. It can be seen that ductility, as indicated by true strain, increases with decreasing tensile strength.

Finally, it should be said that an important conclusion of this work is that, in terms of mechanical properties, there is no advantage in increasing the amount of Widmanstätten ferrite in a weld deposit. Acicular ferrite has superior mechanical properties to those of Widmanstätten ferrite (Otterberg *et al.*, 1980; Dolby, 1982; Abson and Pargeter, 1986), and yet, as this work shows, has equivalent tensile properties.

5.7 SUMMARY

The strength of the primary regions of a range of low-alloy steel weld metals has

a)

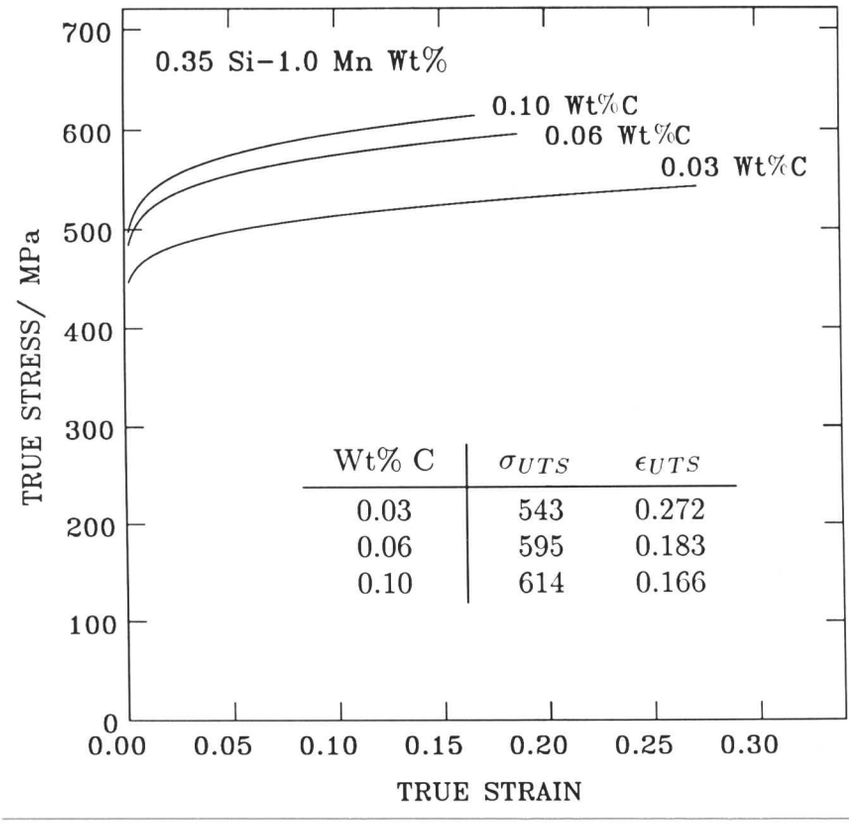

Wt% C	σ_{UTS}	ϵ_{UTS}
0.03	543	0.272
0.06	595	0.183
0.10	614	0.166

b)

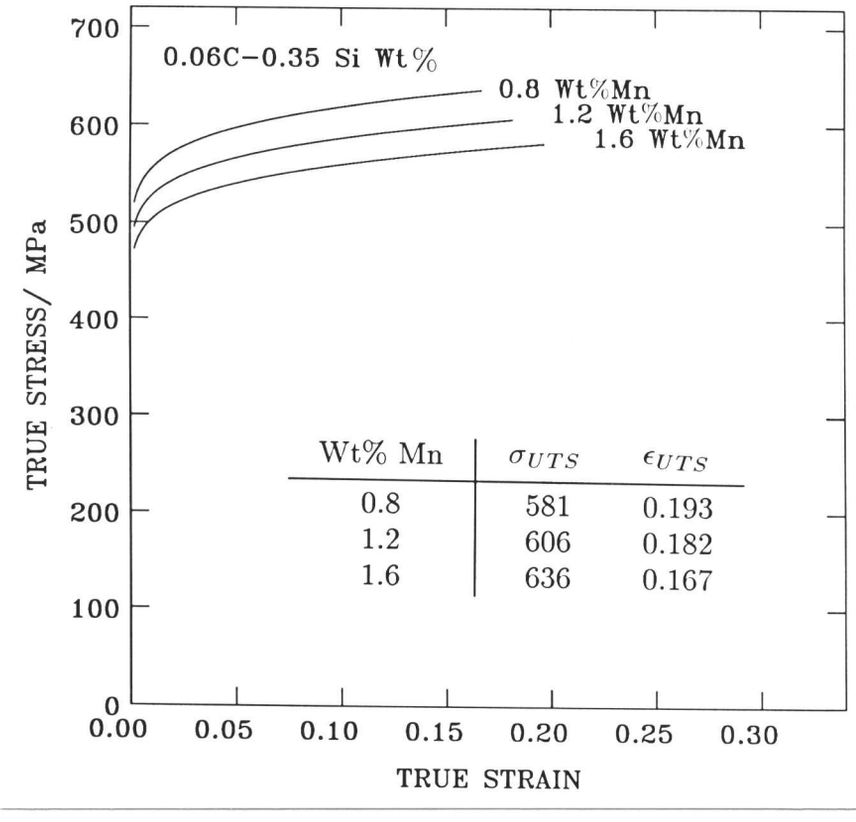

Wt% Mn	σ_{UTS}	ϵ_{UTS}
0.8	581	0.193
1.2	606	0.182
1.6	636	0.167

Figures 5.8a and b: True stress/true strain curves for six hypothetical welds calculated up to the ultimate tensile stress for varying (a) carbon and (b) manganese concentrations. The deposit base compositions are (a) 1.0 wt% Mn-0.35 wt% Si, and (b) 0.06 wt% C-0.35 wt% Si. (Welding conditions are as in Figure 5.7).

been investigated as a function of microstructure and composition. It is demonstrated that the yield strength and ultimate tensile strength may be estimated by summing the strength of pure iron, the solid solution strengthening due to the alloying elements, and a contribution due to microstructure. The microstructural contribution is further factorised into the individual effects of the three phases: allotriomorphic ferrite (α), Widmanstätten ferrite (α_w), and acicular ferrite (α_a). It has been possible to rationalise data from a wide range of welds using a unique set of parameters for the model which describing the flow stress and work-hardening behaviour of the individual phases.

The model has been used to construct true stress/true strain curves for a series of hypothetical welds with a representative range of chemical compositions. Calculated tensile behaviour has been interpreted in terms of the kinetics of microstructural development in the weld deposit. It is suggested that the development of two different empirical carbon equivalent equations, one for very low carbon steels and one for general steels, has come about because of the different kinetic conditions that exist at low carbon concentrations, when a small change in carbon concentration leads to a large change in mechanical properties.

It is noted that increasing the volume fraction of α_w in a weld at the expense of acicular ferrite is undesirable, since this is detrimental to toughness, and yet does not increase the strength of the weld.

REFERENCES

ABSON, D. J., and PARGETER, R. J., (1986) *Int. Met. Revs.*, **31**, 141–194.

AHMAD, Iqbal and BARRANCO, J. M., (1970) *Metall. Trans.*, **1**, 989–995.

ALTSHULER, T. L. and CHRISTIAN, J. W., (1967) *Proc. Roy. Soc.*, **261A**, 253–287.

A. S. M. (1985), A. S. M. Handbook, A. S. M. Committee on Fatigue Crack Propagation, American Society for Metals, Metals Park, OH 44073, 376-402.

BAILEY, N. and PARGETER, R. J., (1978) *Weld. Inst. Res. Rep.*, Welding Institute, Abington, U. K., No. 70/1978/M.

BHADESHIA, H. K. D. H., (1981) *Acta Metall.*, **29**, 1117–1130.

BHADESHIA, H. K. D. H., (1982) *Met. Sci.*, **16**, 167–169.

BHADESHIA, H. K. D. H., (1987) "Review on Bainite in Steels", Phase Transformations 1987, *[Proc. Conf.]*, Institute of Metals, London, U.K., in press.

BHADESHIA, H. K. D. H. and EDMONDS, D. V. (1980), *Met. Sci.*, **14**, (2), 41-49.

BHADESHIA, H. K. D. H. and SVENSSON, L.–E. (1988), *Met. Constr.*, in press.

BHADESHIA, H. K. D. H., SVENSSON, L.–E., and GRETOFT, B., (1985) *Acta Metall.*, **33**, 1271–1283.

BHADESHIA, H. K. D. H., SVENSSON, L.–E., and GRETOFT, B., (1986) "Advances in Welding Science and Technology", *[Proc. Conf.]*, ASM International, Metals Park, OH 44073, S.A.David, Ed., 225-229.

BOSWARD, I. G. and JOHN, R., (1979) "Trends in Steel and Consumables for Welding", *[Proc. Conf.]*, Welding Institute, Abington, U. K., 135–150.

CHILTON, J. M. and KELLY, P. M., (1968) *Acta Metall.*, **16**, 637–656.

CONRAD, H. and FREDRICK, S., (1962) *Ibid.*, **10**, 1013–1020.

CONSIDERE, A. (1885), *Ann. Ponts et Chaussées*, **9**, (6), 574-775.

CUNHA, P. C. R., POPE, A. M., and NOBREGA, A. F., (1982) "Second International Conference on Offshore Welded Structures", *[Proc. Conf.]*, Welding Institute, Abington, U.K., paper 40.

DAVIS, A., and SCALA, E., (1973) "Failure Modes in Composites", Istvan Toth, Ed., *[Proc. Conf.]*, The Metallurgical Society of AIMMPE, New York, 81–101.

DIETER, G. E., (1976) "Mechanical Metallurgy", 2^{nd} Ed., McGraw-Hill, 82.

DOLBY, R. E. (1982), "Advances in the Physical Metallurgy and Applications of Steels", *[Proc. Conf.]*, 111-125.

DOWLING, J. M., CORBETT, J. M., and KERR, H. W. (1986), "Inclusions and Residuals in Steels: Effects on Fabrication and Service Behaviour", *[Proc. Conf.]*, Canadian Government Publishing Centre, Ottawa, Canada, 469-486.

EASTERLING, K. E. (1983), "Introduction to the Physical Metallurgy of Welding", Butterworths & Co., London, U.K., 111.

EVANS, G. M., (1981) IIW Doc. II-A-546-81.

FUKUDA, H., CHOU, T. W., and KAWATA, K., (1981) "Composite Materials", *[Proc. Conf.]*, Applied Science Publishers Ltd., Barking, U. K., 181–193.

HANSEN, M., (1958) "Constitution of Binary Alloys", McGraw-Hill Book Company, New York, 358–362.

HAYES, J. G., (1974) *Bull. Inst. Maths. Applics.*, **10**, 142–152.

IRVINE, K. J. and PICKERING, F. B., (1963) *J. I. S. I.*, **201**, 518–531.

ITO, Y. and BESSAYO, K. (1968), IIW-Doc. IX-576-68.

JUDSON, P. (1982), "2nd International Conference on Offshore Welded Structures", *[Proc. Conf.]*, Welding Institute, Abington, U.K., Paper 3.

KELLY, A., (1966) "Strong Solids", 1^{st} Ed., Oxford University Press, London, U. K., 139–147.

KIMURA, H., MATSUI, H., TAKAKI, S., KIMURA, A., and OGURI, K., (1981) "Mechanical Properties of BCC Metals", *[Proc. Conf.]*, The Metallurgical Society of AIME, Warrendale, Pa. 15086, Ed., M. Meshii, 125–133.

KITAJIMA, K., AONO, Y., ABE, H., and KURAMOTO, E., (1979) "Strength of Metals and Alloys", *[Proc. Conf.]*, Pergamon Press, Oxford, U. K., P.Haasen, Ed., 1979, **2**, 965–970.

LACY, C. E. and GENSAMER, M. (1944), *Trans. A. S. M.*, **32**, 88-105. (Discussion 105-110).

LESLIE, W. C., (1972) *Metall. Trans.*, **3**, 5–26.

McROBIE, D. E. and KNOTT, J. F. (1985), *Mat. Sci. Tech.*, **1**, (5), 357-365.

NADAI, A., (1931) "Plasticity", McGraw-Hill Book Co., New York.

NORSTROM, L. -Å., (1976) *Scand. J. Metall.*, **5**, 159–165.

OLDLAND, R. B. (1985), *Aust. Weld. Res.*, (12), 31-43.

OTTERBERG, R., SANDSTROM, R., and SANDBERG, A. (1980), *Met. Tech.*, (10), 397-408.

POWELL, M. J. D. (1970), A Hybrid Method for Nonlinear Algebraic Equations, in "Numerical Methods for Nonlinear Algebraic Equations", Ed., P. Rabinowitz, Gordon and Breach, U.S.A.

SAMUEL, Fawzy H. (1984), *Metall. Trans. A*, **15A**, (10), 1807-1817.

STEEL, A. C., (1972) *Weld. Res. Int.*, **2**, 37–76.

STRANGWOOD, M. and BHADESHIA, H. K. D. H., (1986) "Advances in Welding Science and Technology", *[Proc. Conf.]*, ASM International, Metals Park, OH 44073, S.A.David, Ed., 209–213.

SVENSSON, L–E., GRETOFT, B., and BHADESHIA, H. K. D. H., (1986) *Scand. J. Metall.*,bf 15, 97–103.

TAKEUCHI, S., (1969) *J. Phys. Soc. Japan*, **27**, 167–169.

TAKEUCHI, S., YOSHIDA, H., and TAOKA, T., (1968) Supplement to *Trans. Japan Inst. Metals*, *[Proc. Conf.]*, **9**, 715–719.

TOMOTA, Y., KUROKI, K., MORI, T., and TAMURA, I. (1976), *Mater. Sci. Eng.*, **24**, 85-94.

TWEED, J. H. and KNOTT, J. F., (1987a) *Met. Constr.*, **19**, 153–158.

TWEED, J. H. and KNOTT, J. F. (1987b), *Acta Metall.*, **35**, (7), 1401-1414.

WIDGERY, D. J. (1976), *Weld. J.*, **55**, (3), Weld. Res. Supp., 57s-68s.

YANG, J. R. and BHADESHIA, H. K. D. H., (1986) "Advances in Welding Science and Technology", *[Proc. Conf.]*, ASM International, Metals Park, OH 44073, S.A.David, Ed., 225-229.